Nigerian Research Journal of Engineering and Environmental Sciences 5(2) 2020 pp. 659-671

Nigerian Research Journal of Engineering and Environmental Sciences
Journal homepage: www.rjees.com

Original Research Article

Production and Characterisation of Porcelain Insulator Modified with Talc and Bentonite

***Mgbemere, H.E., Obidiegwu, E.O. and Oginni, A.A.**

Department of Metallurgical and Materials Engineering, University of Lagos, Lagos, Nigeria.
*hmgbemere@unilag.edu.ng; eobidiegwu@unilag.edu.ng; detounoginni@gmail.com

ARTICLE INFORMATION

Article history:
Received 03 Jul, 2020
Revised 02 Oct, 2020
Accepted 09 Oct, 2020
Available online 30 Dec, 2020

Keywords:
Porcelain
Slip casting
Insulators
Talc
Properties

ABSTRACT

Talc and bentonite were used in this research to modify the properties of porcelain insulators. Ball clay, kaolin, feldspar, quartz, talc and bentonite were weighed, milled and slip cast to produce the samples. Sintering was carried out at 1100 ^oC for 2 h in an electric furnace. The samples were characterized using X-ray fluorescence, X-ray diffraction, scanning electron microscopy, Mechanical, physical and electrical properties tests. The chemical analysis showed that SiO_2 was the major constituent in both the raw materials and porcelain. Linear shrinkage in the samples ranged from 5.5 to 8%, and bulk density from 1.8 g/cm^3 to 2.3 g/cm^3. Albite and quartz were the main phases in the XRD patterns while the morphology of the samples revealed relatively dense microstructures containing two distinct phases. The compressive stress-strain graph results showed that the modulus values range from 314 MPa for samples without talc to 566 MPa for the sample with the highest talc content. The electrical tests show that the breakdown voltage ranged from 100 to 150 kV while the leakage current values varied from 1.5 mA to 5 mA. The results indicate that while talc addition helped to increase the compressive modulus values and breakdown voltage, the leakage current values also increased. It can be inferred that while talc addition helped to lower the sintering temperature of porcelain, it also helped to slightly increase the leakage current characteristics of porcelain.

1. INTRODUCTION

Porcelain insulators usually have good mechanical strength and help to provide electrical insulation as well as environmental protection to overhead electrical appliances. One of the advantages of this type of insulators is that they can be used in harsh environments without negatively impacting their properties compared to other types of insulators (Holtzhausen and Vosloo, 2015). The major constituents of the raw materials used

in producing porcelain are usually kaolin, feldspar and quartz and they serve different purposes. Kaolin and other clay minerals help to provide plasticity; feldspar acts as a fluxing agent while quartz gives stability to the porcelain by reducing the rate of shrinkage (Murad and Wagner, 1998; Kitouni and Harabi, 2011; Mgbemere et al., 2019).

Research into porcelain materials is not new as a lot of articles have been published with different combinations of raw materials. In some of these reports, only quartz, feldspar and clay were used. A breakdown voltage of 26 kV/mm, linear shrinkage of 6.6%, apparent porosity of 10.37%, bulk density of 1.79 g/cm^3 and water absorption of 5.49% was reported when 45% kaolin, 5% ball clay, 25% feldspar and 25% quartz were used (Ajakor et al., 2015). A resistivity value of 1.97×10^9 Ωcm, breakdown voltage of 26 kV/mm, 0% water absorption coefficient and dielectric constant between 9.2 and 10.8 was reported using 30% kaolin, 10% ball clay, 22% feldspar and 38% quartz (Anih, 2005). When the clay content was 50%, the properties of the porcelain were enhanced (Okolo et al., 2015; Okolo et al., 2016). Calcination prior to sintering have been reported to improve bulk density values from 1.9 g/cm^3 to 2.32 g/cm^3 for samples containing 37 wt.% kaolin, 35 wt.% feldspar and 28 wt.% quartz (Kitouni and Harabi, 2011). Using the extrusion method, porcelain production has yielded samples which exhibited flashover voltages of 20.3 kV (dry) and 9.3 kV (wet) respectively, transverse strength of 12.5 kN and bulk density of 2.27 g/cm^3 using ball clay (13%) from Mukono, kaolin (27%) and feldspar (40%) from Mutaka and silica (20%) from Lido beach on the shores of Lake Victoria in Entebbe, Uganda (Olupot et al., 2013). Moyo and Park (2014) used Pugu kaolin (48 wt.%), quartz (46 wt.%) and Kilimanjaro feldspar (6 wt. %) to make six different porcelain compositions. The compressive modulus values ranged from 9.42 to 53.525 MPa, bulk density values between 2.23 and 2.31 g/cm^3, apparent porosity from 11.5% to 12.7% depending on temperature of sintering, water absorption from 0.11 to 1.24%, linear shrinkage from 9.5 to 13% and insulation resistance from 10.4 GΩ to 42.7 GΩ.

Other literature reports have in addition to the usual raw materials, introduced new materials in order to modify the properties of the porcelains. Atanda et al. (2012) produced four different porcelain compositions using clay minerals from Ikere Ekiti. Bentonite and calcium carbonate were added in small quantities and the results showed that Ikere Ekiti kaolin had the highest purity and porosity values of 23 – 28.5%, bulk density 1.84–2.1 g/cm^3 and compressive strength 2.55 – 2.69 N/mm^2. Fly ash used to substitute quartz resulted in a microstructure containing quartz grains and secondary mullite needles embedded in feldspathic glassy matrix (Dana et al., 2004). Increasing the sintering temperature led to an increase in linear shrinkage from 6.5% to 11.5%; bulk density between 2.02 and 2.14 g/cm^3 and apparent porosity between 16 and 25%. Different amounts of Al_2O_3 and SiO_2 used to produce porcelain have resulted in high dielectric strength of 97 kV/mm while the microstructure revealed dense, uniform distribution of long and thin needle-shaped mullite grains (Sedghi et al., 2014). As the quartz content in porcelain decreased, the density values increased from 2.3 g/cm^3 to 2.57 g/cm^3 while the porosity of the samples decreased from 3.32% to 0.09%. Talc has also been added to the major raw materials in the production of porcelain (Nwachukwu and Lawal, 2018). Lowering the kaolin content resulted in an increase in the following properties; linear shrinkage from 2.6% to 8.7%; water absorption from 2.52 to 3.72%; bulk density from 2.14 g/cm^3 to 2.74 g/cm^3 and failing load from 1.92 to 2.73 kN. The effect of using different fluxes (nepheline syenite, Talc, manganese dioxide, and barium carbonate) on the properties of electrical porcelain containing 30% Al_2O_3 have been investigated (Sedghi et al., 2012). Density values between 2.62 - 2.7 g/cm^3; bending strength 1475 – 1608 kg/cm^2 and electrical strength of 34 kV were obtained. Zirconia has also been used to modify the properties of porcelain with improved mechanical strength (Jawale et al., 2016).

Talc is a flux which helps to reduce the effective sintering temperatures, enhance mechanical properties as well as improve the gloss finishing of porcelain. In this research, talc and bentonite were introduced to the main constituents of electrical porcelain. The objective of this research was to understand how the sintering temperature of the porcelain can be reduced while maintaining relatively high electrical and mechanical properties in the porcelain insulators.

2. MATERIALS AND METHODS

2.1. Sample Preparation

The starting materials used in this research include ball clay, kaolin, feldspar, silica, bentonite and talc. The raw materials were obtained as coarse powders and had to be milled. Milling was carried out for 5 hours using a ball mill in order to reduce the average particle size of the powders. They were then sieved with a sieve of mesh size 80 µm to obtain particle less than 80 µm. Slip casting was used to obtain the body formulations for casting. To achieve this, 2 g of sodium silicate (Na_2SiO_3) was added to ensure that the slip was deflocculated before pouring into the mould. The preparation of the slip for each composition was achieved by adding 10 cl of distilled water to the mixture. The poured slip began to form a solid layer on the surface of the mould which evacuates through capillary forces (Nwachukwu and Lawal, 2018).

2.2. Composition Formulation

Six different compositions of the porcelain were formulated and wet milled for 5 hours to produce slurry that was suitable for casting. The body formulations are shown in Table 1. The notations A, B, C, D, E and F will subsequently be used to describe the samples. The slip was sieved with a mesh sieve of size 80 µm and then poured into a plaster of Paris mould prepared specifically for the research. The slip in the mould was continuously filled for about 1 h to allow the shape to completely form. The cast was removed after drying in the mould. The rough edges of the cast samples were fettled to improve the surface finish. It was then oven dried at 110 ^oC for 48 h to ensure that the moisture present has been removed. Bisque firing of the samples was carried out at 900 ^oC to remove any carbonaceous part and improve the mechanical properties (Olupot et al., 2013; Ezenwabude and Madueme, 2015).

Table 1: Porcelain body compositions used for slip casting

Sample	Kaolin wt. (g)	Feldspar wt. (g)	Quartz wt. (g)	Bentonite wt. (g)	Ball Clay wt. (g)	Talc wt. (g)
A	600	300	400	100	600	0
B	300	300	400	100	900	0
C	590	290	390	90	590	50
D	580	280	380	80	580	100
E	570	270	370	70	570	150
F	560	260	360	60	560	200

2.3. Glaze Formulation

The surfaces of the samples were cleaned in preparation for glazing. The composition of the glaze used is shown in Table 2.

Table 2: Composition of the materials used in glazing the electrical porcelain

Materials	Percentage usage (%)
Ball clay	35
Kaolin	19.5
Potassium feldspar	19
Manganese oxide	5
Cobalt	1
Chrome oxide	0.5
Lithium carbonate	15
Iron oxide	5
Total	100

The pictures showing the unfettled samples, glazed samples before and after firing are shown in Figure 1. The glaze was applied on the surface of the bisque-fired samples by dipping and placing on a graduated cylinder. The dipping process was carried out twice with the second dip coming 30 secs after the first dip. The samples were allowed to dry and then sintered/glazed in a vertical position inside an electric kiln at 1100 ^{o}C for 2 hours at a heating rate of 5 ^{o}C/min. The samples were left in the kiln for about 10 hours to cool to room temperature.

Figure 1: Pictures showing the unfettled samples, glazed samples before and after firing in the furnace

2.4. Sample Characterisation

The chemical composition analyses of the starting raw materials were carried out using an X-ray fluorescence analyser (Venarum Mines Laboratory Apapa, Lagos). The analysis of the powders was carried out twice using 1 g each of the powders. The linear shrinkage in the sintered samples was determined according to ASTM C356-17 standard by measuring the dimensions of the samples before and after sintering and then using the relation in Equation 1 to determine the shrinkage values (Atanda et al., 2012; Nwachukwu and Lawal, 2018).

$$Linear\ Shrinkage = \frac{L_w - L_f}{L_w} \times 100 \quad (1)$$

where L_w = length before sintering, L_f = length after sintering
The apparent porosity in the samples was also determined in accordance with ASTM_C20-00 standard by first measuring the dry mass and then immersing the sample in water for 10 h after which the weight of the soaked specimen was taken (Atanda et al., 2012). The formula used to determine the apparent porosity is shown in Equation 2.

$$Apparent\ Porosity = \frac{W_a - W_b}{W_a} \times 100 \quad (2)$$

Where W_a = weight after immersion, W_b = weight before immersion

The density of the samples was measured using Archimedes method which is based on the principle of upthrust (Dana et al., 2004). The formula used is shown in Equation 3.

$$Density = \frac{M_{BP} - M_B}{V_P} \quad (3)$$

Where D is density of porcelain (g/cm^3), M_{BP} the mass of container and porcelain (g), M_B the mass of container only (g) and V_P the volume of the porcelain (cm^3) (Nwachukwu and Lawal, 2018).

This was done by measuring the weight of the dry sample and then suspending the sample in a beaker filled with distilled water and taking the measurement. The sample was subsequently dried and re-weighed. Three samples of the same composition were tested and the average value was recorded.

The compressive strength test was carried out using a compression testing machine (Instron 3369, USA). The samples were cylindrical in shape with a cross sectional area of ~ 630 mm^2. The samples were put in the machine and progressively compressed until failure. The compressive stress was obtained by calculating the ratio of maximum load as a function of the cross-sectional area. To determine the morphology of the samples, a scanning electron microscope (Carl Zeiss, Jena Germany) image of the samples was obtained. The microscope has an energy dispersive spectroscopy analyser operating at 15 kV (Smart Quant Instruments) attached to it. The samples were initially sputtered with gold to ensure that there was adequate electrical contact. A high vacuum (10^{-6}) was generated in the system before the measurements were carried out.

The X-ray diffraction analysis was carried out using an X-ray diffractometer (EMPYREAN, Nigerian Geological Survey Agency, Kaduna.) with a *Cukα* radiation operating at 45 kV and 40 mA. The scan angle is from 5^o to 75^o with a continuous scan step of 0.026^o. The samples were ground into powders and put inside the machine. The insulation property of the samples was determined using a high voltage transformer (Hivotech Laboratory, University of Lagos). The samples were prepared by applying electrodes at both ends of the samples. The voltage in the samples was gradually increased and the onset of spark as well as the breakdown voltage in the samples was obtained.

3. RESULTS AND DISCUSSION

3.1. X-ray Fluorescence Analysis

The results of the chemical composition analyses for all the starting raw powders are shown in Table 3. The major compound present in all the starting powders was SiO_2. The results also indicate that since the starting materials came from nature, they also contain considerable amounts of associated impurity compounds.

Table 3: The chemical composition of the raw materials used in producing the porcelain insulator

Compound	Talc	Quartz	Feldspar	Ball clay	Kaolin	Bentonite
SiO_2 (wt.%)	57.78	90.38	64.19	44.64	46.53	48.21
MgO (wt.%)	28.65	-	0.07	4.06	0.002	0.91
CaO (wt.%)	2.91	0	0.24	-	0.28	2.32
Al_2O_3 (wt.%)	0.82	1.62	20.37	41.13	39.19	36.44
Fe_2O_3 (wt.%)	2.39	0.37	0.15	11.25	0.62	9.08
K_2O (wt.%)	1.22	0.01	2.38	2.32	0.17	0.18
TiO_2 (wt.%)	0.04	0.02	0.2	1.07	3.05	0.29
Na_2O (wt.%)	0.35	<0.001	1.49	8.11	0.19	0.11
BaO (wt.%)	0.01	-	0.13	-	0.001	0.52
MnO (wt.%)	0.05	0.01	-	0.48	0.21	0.31
P_2O_5 (wt.%)	0.06	0.01	-	-	-	-
CuO (wt.%)	3.67	-	-	-	-	-
PbO (wt.%)	-	-	-	0.03	-	0.14
ZnO (wt.%)	-	-	-	2.11	0.003	-
LOI	2.05	7.58	10.78	-15.2	9.754	1.49

Talc was the main source of MgO in the porcelain with 28.65% content while other impurity compounds contributed 11.52%. The impurities in quartz amounted to 2.04%. Feldspar, ball clay, kaolin and Bentonite

were the main sources of Al_2O_3 contributing 20.37%, 41.13%, 39.19% and 36.44% respectively. Other impurities that are present in the raw materials are MgO, CaO, Fe_2O_3, K_2O, TiO_2, Na_2O, BaO, MnO, CuO and ZnO. A comparison of this result with others in the literature indicates that they are similar. It must be noted however that composition varies from location to location due to weather and differences in climatic conditions of the area where these minerals are found. They are either slightly lower or higher compared to literature reports. The SiO_2 content in quartz, feldspar, ball clay and kaolin were slightly lower in the following references (Dana et al., 2004; Kitouni and Harabi, 2011) while that in Nwachukwu and Lawal, (2018) were higher compared to the ones in this report.

3.2. X-ray Diffraction

The X-ray diffraction patterns of the samples as a function of compositions are shown in Figure 2. The diffraction patterns were matched with already existing patterns in the database. For sample A, Albite ($Na_{1.96}Ca_{0.04}Si_{5.96}Al_{2.04}O_{16}$) (96-900-9664) and quartz (SiO_2) (96-500-0036) were used to adequately describe the diffraction pattern with the former contributing 18% while the later contributed 65% to the pattern. For sample B, quartz and Albite ($Na_2Al_2Si_6O_{16}$) (96-900-1633) were also used to match the obtained pattern. The obtained score for each phase is 50 and 10 % respectively. For sample C, Quartz and Albite ($Al_2Si_6Na_2O_{16}$) (96-900-1631) were also matched the obtained pattern. The obtained score for each phase is 54 and 4 % for each phase respectively. For sample D, quartz and Albite ($Na_{1.96}Ca_{0.04}Si_{5.96}Al_{2.04}O_{16}$) (96-900-9664) were also used to match the obtained pattern. The obtained score for each phase is 78 and 11 % respectively. For sample E, quartz and Albite ($Na_{1.96}Ca_{0.04}Si_{5.96}Al_{2.04}O_{16}$) (96-900-9664) were also used to match the obtained pattern. The obtained score for each phase is 56 and 14 % respectively. For sample F, quartz, Albite ($Na_{1.96}Ca_{0.04}Si_{5.96}Al_{2.04}O_{16}$) (96-900-9664) and Sillimanite ($Al_8Si_4O_{20}$) (96-900-6528) were also used to match the obtained pattern. The obtained score for each phase is 51, 15 and 12 % respectively. Quartz and mullite have been reported to be the crystalline phases present in triaxial porcelain (Olupot, 2006; Kitouni and Harabi, 2011; Olupot et al., 2013).

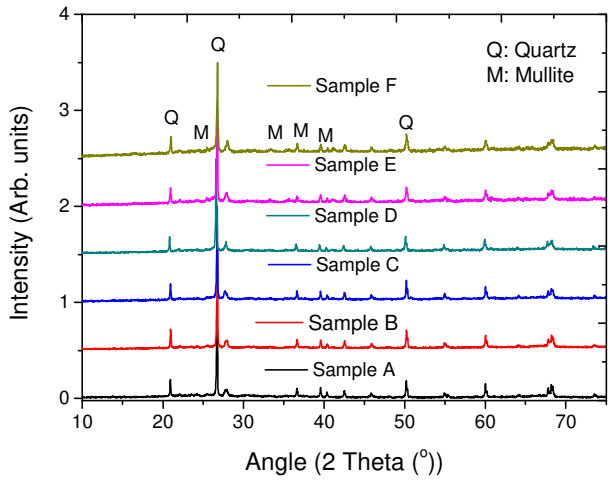

Figure 2: X-ray diffraction patterns of electrical porcelain insulators as a function of talc and bentonite amount

3.3. Scanning Electron Microscopy

The scanning electron microscope images as well as their corresponding energy dispersive X-ray spectroscopies are shown in Figure 3. Dense microstructures with some porosity were observed for the samples except in sample E which has a clear porous morphology. Dark and light features are observed on the surfaces of the samples possibly corresponding to albite and silica phases which can be seen with the

XRD. Very little glass phase could be observed on the micrograph. The microstructure of porcelain samples has been reported to contain quartz and mullite phases which are surrounded by glassy matrix of elongated mullite crystals (Dana *et al.,* 2004). The possible explanation for the low amount of glassy phase could be due to the sintering at 1100 ^{o}C which is adequate to densify the samples and formed some glassy phase. A look at the graph of density values in figure 5 shows that they are in the same range. This is corroborated by the microstructures which have the same morphology. As the amount of talc in the samples increased, the formation of the glassy phase becomes common (Sedghi et al., 2012). This statement agrees with the assertion that the amount flux and sintering temperature determines the amount of glass phase formed. Temperatures of 1250 ^{o}C and above are known to be the optimum for sintering porcelain which gives good mechanical characteristics (Olupot et al., 2013).

The light phases appear at the grain boundaries and are most probably the quartz phase. The EDX of the samples revealed the presence of the two dominant peaks for Si_k and Al_k. This is similar to the result from the chemical analysis where the major elements present are Si and Al. Smaller peaks for the minor elements K, Ca, Ti, Fe etc. could also be detected. A quantitative EDX analysis was also carried out and the result is shown in Table 4. As the amount of talc increased, the intensity of the Al and Si peaks also increased. The quantitative EDX result showed that after the sintering process, the composition of the Si and Al appear to converge at approx. 55% while that of Al is between 23 and 29%. The content of K increased with increasing talc content while that of Ti decreased. New elements which were not identified in the raw powders were also observed. This could possibly due to the porcelain coming in contact with these elements during processing.

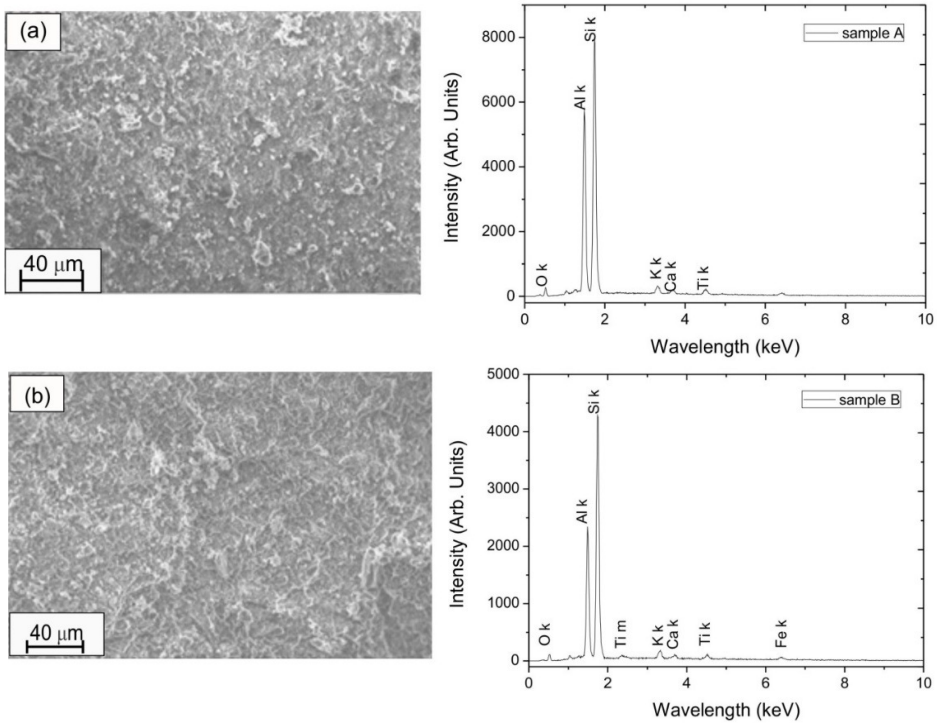

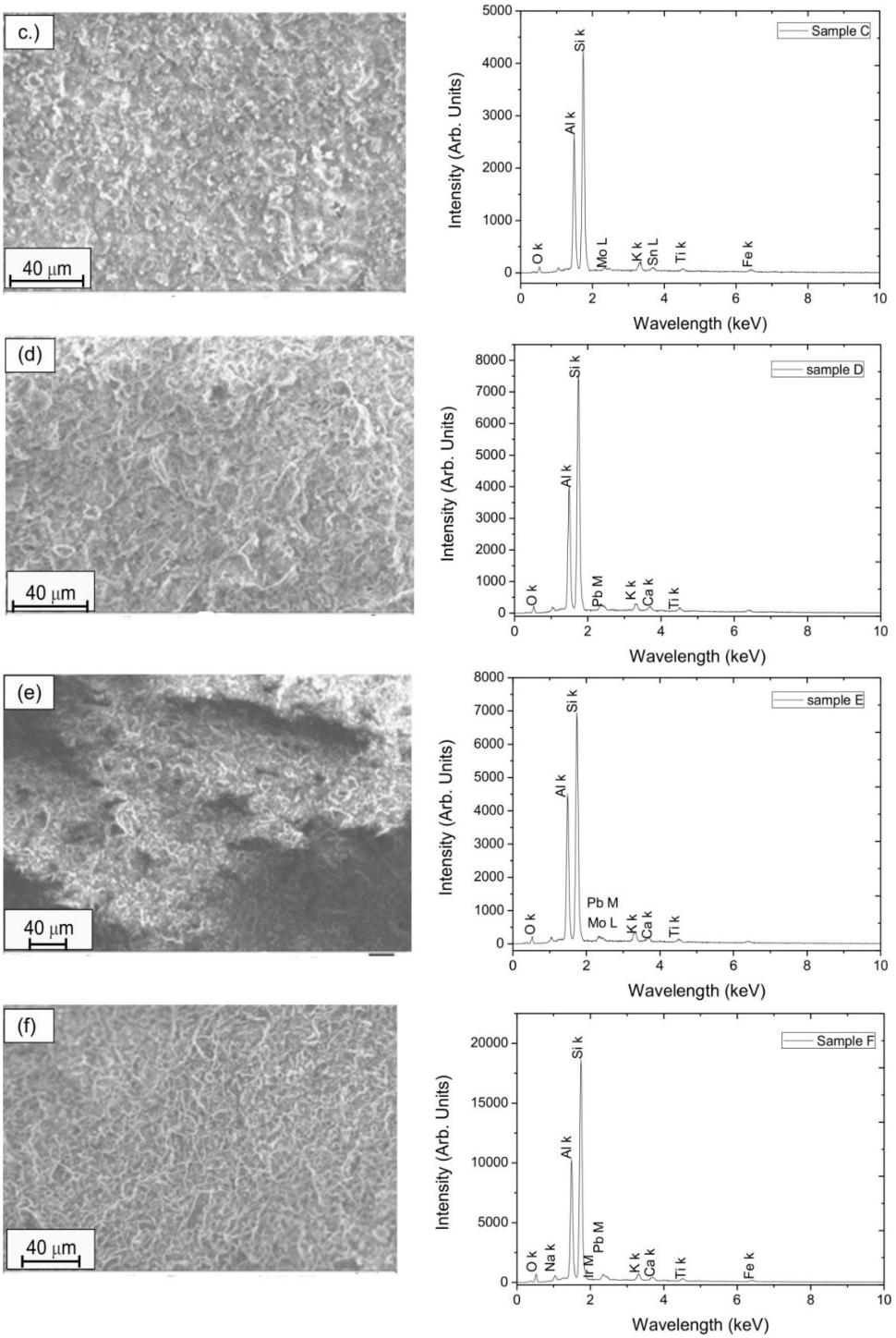

Figure 3: Scanning electron microscope images and the corresponding energy dispersive spectroscopy of electric porcelain insulators

Table 4: Table showing the results of quantitative EDX carried out on the electrical porcelain

Element	Sample A	Sample B	Sample C	Sample D	Sample E	Sample F
	Amount (wt. %)					
O K	3.04	2.15	2.15	2.41	2.78	4.32
Al K	29.2	23.27	26.21	23.43	26.75	23.1
Si K	57.62	59.59	58.8	59.3	56.02	54.39
K K	3.76	3.78	4.49	4.05	5.42	3.99
Ca K	2.41	1.9	-	2.91	2.76	2.76
Ti K	3.97	3.33	2.14	2.81	2.81	2.31
Fe K	-	5.79	4.37	-	-	2.99
Tl M	-	0.19	-	-	-	-
Mo L	-	-	1.1	-	0.7	-
Sn L	-	-	0.74	-	-	-
Pb M	-	-	-	5.08	2.77	4.96
Na K	-	-	-	-	-	0.24
Ir M	-	-	-	-	-	0.94

3.4. Linear Shrinkage and Apparent Porosity

The linear shrinkage and apparent porosity values of the samples as a function of sample compositions is shown in Figure 4. The effect of the clay minerals is analysed in Samples A and B. When the same amount of kaolin and ball clay was used to produce the porcelain, the linear shrinkage value of 5.5% was obtained. When the amount of kaolin was reduced while the ball clay content was increased by the same amount, the linear shrinkage increased to 6.3%. This is an indication that the more plastic the sample is, the higher is the shrinkage. As the amount of other constituents is lowered while increasing the talc content, the shrinkage rate initially increases to 7.4%. As the talc content increases further, the shrinkage rate decreases to 5.6%. As the talc content continues to increase, the linear shrinkage also increases. The values from this study closely resemble reports in the literature for porcelain insulators. A shrinkage value of 6.6% was reported by Ajakor et al. (2015) while shrinkage rates from 3 to 8.7% was reported by Nwachukwu and Lawal, (2018). As the amount of talc in the porcelain increased, the apparent porosity in the samples decreased from 14.23±2.4 % to 12±1.9 %. This implies that talc helps to decrease the porosity in the sample which corresponds to slight increase in the density values.

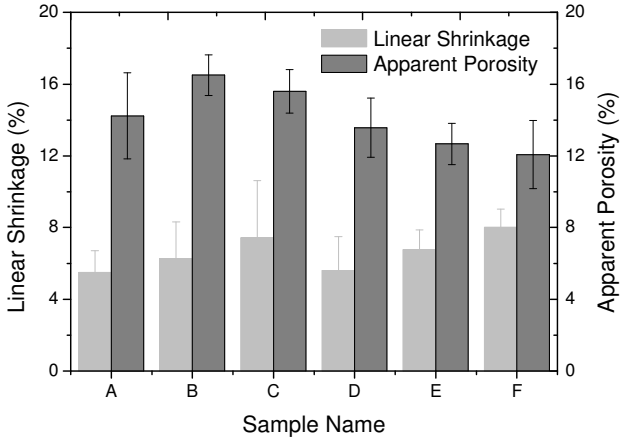

Figure 4: Graph of linear shrinkage (%) and apparent porosity (%) as a function of sample composition.

3.5. Bulk Density

The plot of the bulk density of the samples as a function of composition is shown in Figure 5. Statistically there is no difference in the density values of the samples irrespective of composition. For samples A and B which did not contain talc, when the amounts of kaolin and ball clay are the same, the density values were 2.16±0.09 g/cm^3 and 1.98±0.12 g/cm^3 respectively. This implies that the presence of kaolin leads to improved densification of the sample which in turn leads to higher density value (Mgbemere et al., 2019). In another report, the density of the porcelain increased when feldspar and quartz contents were increased (Nwachukwu and Lawal, 2018). For samples C to F, the density values follow similar trends to that of linear shrinkage. When talc was introduced, the density initially increased to 2.21±0.19 g/cm^3 and with further increment, decreased to 2.03±0.04 g/cm^3. Further additions of talc and reductions in the other constituents resulted in an increase in the density values. This is possibly due to the fact that as a flux, the higher its content, the lower will be the activation energy for sintering and densification. A density value of 1.79 g/cm^3 has been reported for triaxial porcelain (Ajakor et al., 2015). When flyash was used to substitute triaxial porcelain at a sintering temperature of 1100 ºC, the density values were between 2.03 and 2.13 g/cm^3 (Dana et al., 2004). For triaxial porcelain alone sintered at 1100 ºC, the bulk density was 2.23 g/cm^3 for sample without prior calcination and 1.7 g/cm^3 for calcined samples (Kitouni and Harabi, 2011). It can be inferred from this that density depends on many factors including composition as well as processing parameters.

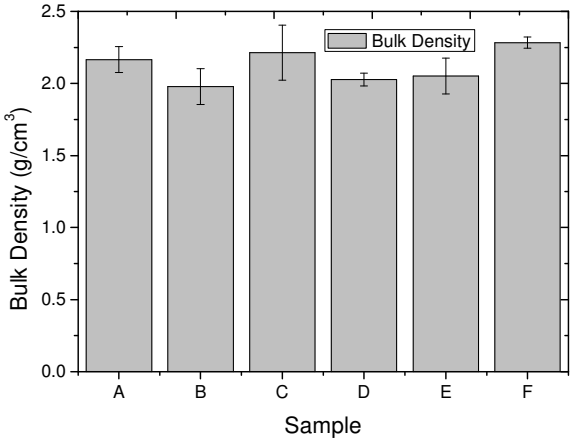

Figure 5: Graph of bulk density as a function of sample composition

3.6. Compressive Strength

The plot of compressive stress as a function of compressive strain for the samples is shown in Figure 6. The slope of the stress-strain graph was used to calculate the compressive modulus for the samples. The results show that as talc was introduced to the samples, the values of compressive modulus increased. For sample A and B, the compressive moduli have been calculated to be 314.56±9.08 MPa and 352.68 ± 10.28 MPa respectively. When talc is introduced (sample C), the modulus value increased to 507.69±5.5 MPa. A slight decrease in modulus was observed as more talc (sample D) was added with the value decreasing to 417.06±8.25 MPa. The modulus values increased to 559.46 ±17 MPa and 566 ± 9.52 MPa for samples E and F respectively with increasing talc content. From this result, it can be inferred that as more talc is introduced, the samples increased in density which in turn leads to higher compressive modulus and by extension mechanical strength.

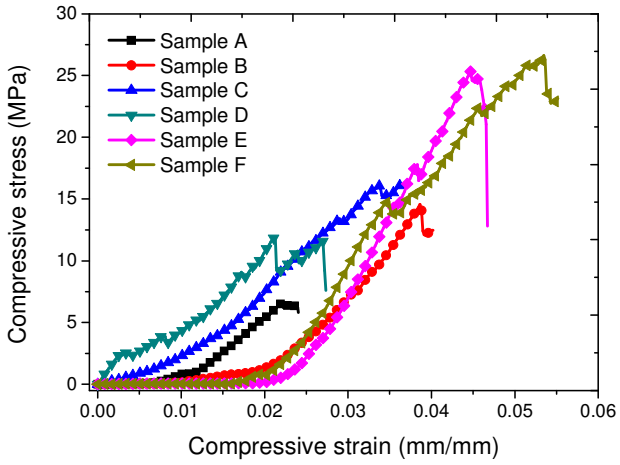

Figure 6: A graph of compressive stress as a function of compressive strain for electrical porcelain insulators

3.7. Electrical Properties

The result of the electrical tests on the electrical porcelain samples namely; the withstand voltage, inception voltage, breakdown voltage and leakage current are shown in Table 5. The inception voltage represents that lowest voltage where a partial discharge occurs in a small part of the device subjected to high voltage while withstand voltage is that voltage the insulator material can withstand in still air for about 3 minutes at room temperature. The withstand voltage was obtained in the samples when the minimum voltage reached up to 70 kV. A similar trend was observed when other measurements were carried out. As more talc was introduced, the withstand voltage increased to 82 kV from 70 kV when there was no talc present. With subsequent talc addition, the value decreases to 70 kV and gradually increases to 85 kV. The inception voltages are highest both with and without the highest Talc content. As talc is introduced, the voltage increased from 90 kV corresponding to the least content to 100 kV when it is highest. The addition of talc to the insulator clearly improved the breakdown voltage values but also resulted in higher leakage current values. The reason for this can be that as talc content in the porcelain increased, the number of electrical conduction sites also increased. The impulse breakdown voltage of an 11 kV porcelain insulator has been reported to be 110 kV (Ezenwabude and Madueme, 2015) while the flashover voltage under dry conditions for an insulator is 75 kV. The values obtained from this research are higher and implies that the produced porcelain is suitable for insulator applications.

Table 5: The properties of electrical porcelain insulators

Sample	Withstand voltage (kV)	Inception voltage (kV)	Breakdown voltage (kV)	Leakage current (mA)
A	85	100	150	1.5
B	70	90	110	4
C	82	90	100	3
D	70	95	120	4
E	84	95	130	4
F	85	100	140	5

The graph of both breakdown voltage and leakage current as a function of sample composition is shown in Figure 7. When there was no talc present in the samples (sample A), the highest breakdown voltage (150 kV) value was obtained. As the amounts of kaolin and ball clay were varied, the breakdown voltage decreased to 110 kV (sample B). The leakage current is also lowest (1.5 mA) with the sample containing equal amounts of the kaolin and ball clay. The breakdown voltage lowered to 100 kV when talc was introduced to the samples. As more amounts of talc were added, the breakdown voltage gradually increased up to 140 kV for the sample with the highest content of talc (sample F).

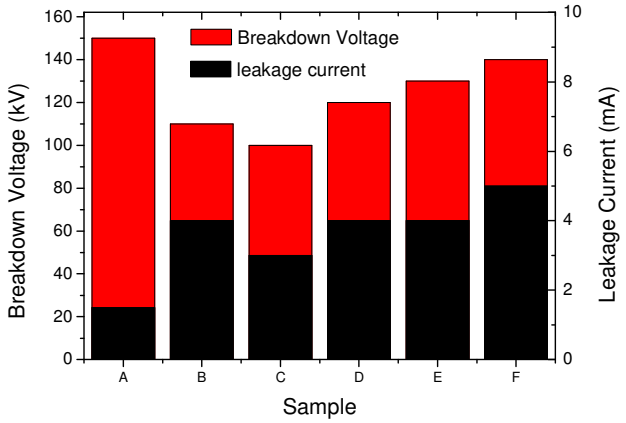

Figure 7: A graph of breakdown voltage against sample composition for the electrical porcelain insulators.

4. CONCLUSION

The effect of adding talc and bentonite on the properties of electrical porcelain insulators have been investigated in this research. The X-ray fluorescence shows that SiO_2 is the major compound present in all the starting powders as well as in the electrical porcelain. The linear shrinkage values in the samples ranged from 5.5% to 8%. The bulk density value ranged from 1.8 g/cm^3 to 2.3 g/cm^3. The X-ray diffraction data shows that albite and quartz are the main phases present in all the samples. The morphology examination indicates that all the samples have dense microstructures with little or no pores. The compressive stress-strain graph result used to determine the compressive modulus gave values from 314 MPa to 566 MPa samples have dense microstructures with little or no pores. The breakdown voltage values show that the values are in the range of 100 to 150 kV are obtained while the leakage current ranges from 1.5 mA to 5 mA. The results show that with the introduction of talc, the mechanical properties of electrical porcelain are enhanced while the electrical properties are slightly lowered. It can be said that the porcelain insulators produced using these compositions can appropriately be used to produce insulators for high voltage applications.

5. ACKNOWLEDGMENT

The authors wish to acknowledge the assistance and contributions of the laboratory staff (especially Mr. Obe Yekini Johnson) of Ceramics Department at the Federal Institute of Industrial Research Oshodi (FIIRO) toward the success of this work.

6. CONFLICT OF INTEREST

There is no conflict of interest associated with this work.

REFERENCES

Ajakor, E. M., Anih, L. U. and Ogwata, C. M. (2015). Indigenous Production of Electrical Porcelain from Nigerian Mineral. *International Journal of Scientific and Research Publications,* 5(6)**,** pp. 1-3.

Anih, L. U. (2005). Indigenous Manufacture and Characterization of Electrical Porcelain Insulator. *Nigerian Journal of Technology,* 24(1)**,** pp. 1-7.

ASTM C20-00 (2015). Standard Test Methods for Apparent Porosity, Water Absorption, Apparent Specific Gravity and Bulk Density of Burned Refractory Brick and shaped by boiling Water. *ASTM International,* West Conshohocken, PA, www.astm.org.

ASTM C356-17 (2017). Standard Test Method for Linear Shrinkage of Preformed High Temperature Thermal Insulation Subjected to Soaking Heat. *ASTM International*, West Conshohocken, PA, www.astm.org.

Atanda, P. O., Oluwole, O. O. and Oladeji, T. A. (2012). Electrical Porcelain Production From Selected Kaolin Deposit in South Western Nigeria Using Slip Casting. *International Journal of Materials and Chemistry* 2(3)**,** pp. 86-89.

Dana, K., Das, S. and Das, K. S. (2004). Effect of Substitution of Fly Ash for Silica in Triaxial Kaolin Silica Feldspar System. *Journal of the European Ceramic Society,* 24**,** pp. 3169-3175.

Ezenwabude, E. I. and Madueme, T. C. (2015): Investigated the Evaluation of Mixed Local Materials for Low Voltage Insulators. *International Journal of Multi-Disciplinary Sciences and Engineering* 6, p. 37.

Holtzhausen, J. P. and Vosloo W. L. (2015). High Voltage Engineering – Practice and Theory.

Jawale, G., Kumar, N. and Majhi, M. R. (2016). Synthesis and characterization of Zirconia doped Electrical Porcelain Insulator. *International Research Journal of Engineering and Technology,* 3(10)**,** pp. 1-5.

Kitouni, S. and Harabi, A. (2011). Sintering and mechanical properties of porcelains prepared from algerian raw materials. *Cerâmica* 57**,** pp. 453-460.

Mgbemere, H. E., Onyeayana, I. P. and Okoubulu, A. B. (2019). The Effect of Kaolin and Silica variation on the Properties of Porcelain Insulators. *Nigerian Journal of Technology,* 38, pp. 647-653.

Moyo, M. G. and Park, E. (2014). Investigation of the ceramic raw materials in Tanzania – structure and properties for electrical insulation application. *International Journal of Engineering Research & Technology (IJERT),* 4(2)**,** pp. 34-41.

Murad, E. and Wagner, U. (1998). Clays and clay minerals: The firing process. *Hyperfine Interactions,* 117**,** pp. 337-356.

Nwachukwu, V. C. and Lawal, S. A. (2018). Investigating the Production Quality of Electrical Porcelain Insulators from Local Materials. *IOP Conf. Series: Materials Science and Engineering,* 413(012076 1-8).

Okolo, C. C., Ezechukwu, O. A., Olisakwe, C. O., Ezendokwelu, C. E. and Umunna, C. (2015). Characterization of Electrical Porcelain Insulators from Local Clays. *International Journal of Research – Granthaalayah,* 3**,** pp. 26-36.

Okolo, C. C., Anierobi, C. C., Obute, K. C., Ezechukwu, O. A. and Olisakwe, C. O. (2016). Determination of Dielectric Strength of Electrical Porcelain Insulators from local Clays using a Snail Shell as an Additive. *International Journal of Recent Advances in Multidisciplinary Research,* 3(8), pp. 1667-1671.

Olupot, P. W. (2006). Assessment of Ceramic Raw Materials in Uganda for Electrical Porcelain. *Department of Materials Science and Engineering.* Stockholm, Royal Institute of Technology (KTH) Sweden.

Olupot, P. W., Jonsson, S. and Byaruhanga, J. K. (2013). Effects of the Sintering Process on Properties of Triaxial Electrical Porcelain from Ugandan Ceramic Minerals. *International Scholarly and Scientific Research and Innovation,* 7(5)**,** pp. 267-273.

Sedghi, A., Hamidnezhad, N. and Noori, N. R. (2012). The Effect of Fluxes on Alumina Silicate Porcelain Insulator Properties and Structure. *International Conference on Ecological, Environmental and Biological Sciences (ICEEBS'2012)* Dubai.

Sedghi, A., Riahi-Noori, N., Hamidnezhad, N. and Salamani, M. R. (2014). Effect of Chemical composition and alumina content on structure and properties of ceramic insulators. *Bulletin of Materials Science,* 37(2), pp. 321-325.